

# Constraining heavy decaying dark matter with the high energy gamma-ray limits

O. E. Kalashev and M. Yu. Kuznetsov\*

*Institute for Nuclear Research of the Russian Academy of Sciences,  
60th October Anniversary Prospect 7a, 117312 Moscow, Russia*  
(Received 3 July 2016; published 30 September 2016)

We consider decaying dark matter with masses  $10^7 \lesssim M \lesssim 10^{16}$  GeV as a source of ultrahigh energy (UHE) gamma rays. Using recent limits on UHE gamma-ray flux for energies  $E_\gamma > 2 \times 10^{14}$  eV, provided by extensive air shower observatories, we put limits on masses and lifetimes of the dark matter. We also discuss possible dark matter decay origin of tentative 100 PeV photon flux detected with the EAS-MSU experiment.

DOI: [10.1103/PhysRevD.94.063535](https://doi.org/10.1103/PhysRevD.94.063535)

## I. INTRODUCTION

One of the candidates for the role of dark matter is superheavy particles [1,2] (see also Refs. [3,4]), which we will denote as  $X$  particles. From the point of view of particle physics they can be incorporated into various theories (see, e.g., Refs. [5,6] and references therein). In cosmology these particles could be created at some early stages of the Universe evolution [1,2,5–10]. In this paper we consider indirect detection of superheavy dark matter (SHDM). The parameters that can be experimentally constrained in this approach are mass, annihilation cross section, and lifetime of the dark matter particles. While there are several constraints on  $X$  particle mass  $M_X$  imposed by various scenarios of the dark matter production [5,10–13], in this study we conservatively consider the full range of  $M_X$  accessible for indirect observation in recent high energy cosmic ray experiments, namely,  $10^7 \lesssim M_X \lesssim 10^{16}$  GeV. The detection of the annihilation signal of particles with these masses is far beyond reach of the modern experiments because of the unitarity bound on the  $X$  particles annihilation cross section [14]:  $\sigma_{\text{ann}} \sim 1/M_X^2$ . Therefore, in this work we are focusing on the case of decaying DM with long lifetime  $\tau \gg 10^{10}$  yr.

Modern cosmic ray experiments allow one to study primary particle composition based on observed extensive air showers (EAS) properties. The spectrum of protons and nuclei with  $E > 100$  TeV has been studied in detail in several experiments. In contrast, only upper limits on gamma ray fluxes in the same energy range have been obtained so far.<sup>1</sup> In this paper we are using these limits to build constraints on decaying SHDM. For the highest energy ( $E \gtrsim 10^{18}$  eV) the recent constraints on gamma ray flux are given by Pierre Auger Observatory [17,18], Telescope Array experiment [19], and Yakutsk experiment

[20]. Among the constraints of lower energy gamma flux are the results of KASCADE-Grande [21], KASCADE [22], and CASA-MIA [23].

The main motivation for this study is to refine constraints on SHDM parameters using all currently available experimental data. For previous works on the same subject see, e.g., [14,24,25]. In recent years the interest in the subject has grown [26–29] due to petaelectronvolt (PeV) neutrino events observed by IceCube [30].

This paper is organized as follows. In Sec. II we briefly review SHDM decay physics, consider assumptions about source distribution and propagation of photons in a cosmic medium, and calculate the photon flux from the decay of SHDM. In Sec. III we compare our results with existing limits on high energy photon flux and constraint SHDM mass and lifetime.

## II. GAMMA-RAY FLUX FROM SHDM DECAY

The decay of superheavy particles  $X$  was studied in detail in several works [31–35]. In this work we concentrate on QCD decay channels, since in this case a relatively large flux of photons is produced, which makes them easier to constrain with experimental photon flux limits. Note that other decay modes (i.e., leptonic) may also lead to some photon flux either via direct gamma production or by means of interactions of products (i.e., electrons) with cosmic microwave background (CMB) and galactic media. However, these channels may be important only if QCD decay is relatively suppressed. For a review of various DM decay modes see Ref. [36].

We consider the two-body decay into a quark-antiquark or gluon-gluon pair. The following QCD cascade develops down in energy until hadronization occurs. As a result of hadronization and the subsequent decay of an unstable hadron, particles such as protons, photons, electrons, and neutrinos are produced. It is important to note that the impact of electroweak interactions on the hadronic decay channels is subdominant with respect to other uncertainties

\*mkuzn@inr.ac.ru

<sup>1</sup>We should also mention a tentative result of primary gamma detection in the EAS-MSU experiment [15,16].

of this calculation (e.g., the choice of fragmentation functions; see below). For the low  $M_X$ –low energy region we validate this assumption comparing the decay spectra of Refs. [36,37] with and without electroweak (EW) corrections. For high  $M_X$  and high energies we compare the spectra obtained in Refs. [34,35], where full minimal supersymmetric standard model (MSSM) was considered, with that of Ref. [32], where authors considered only supersymmetry (SUSY) QCD interactions. In both energy regions the difference was found to be negligible.

In some earlier works (see, e.g., Ref. [24]) the observed shape of the proton spectrum was also used to constrain the SHDM parameters. This method gives weaker results than the usage of  $\gamma$  limits since the proton flux is dominated by the particles of the astrophysical origin. Therefore in this study we do not consider proton flux from the SHDM decay.

Technically the spectra of the  $X$ -particle decay are defined similarly to the spectra of the  $e^+e^- \rightarrow$  hadrons process [38],

$$F^h(x, s) = \sum_i \int_x^1 \frac{dz}{z} C_i(z, \alpha_s(s)) D_i^h\left(\frac{x}{z}, s\right), \quad (1)$$

where  $x \equiv \frac{2E}{M_X}$  is the energy of the hadron as a fraction of the total available energy,  $D_i^h(x, s)$  are the fragmentation functions of the hadron of the type  $h$  from the parton of the type  $i$ ,  $C_i(z, \alpha_s(s))$  are the coefficient functions, and the summation goes over all types of partons  $i = \{u, \bar{u}, d, \bar{d}, \dots, g\}$ . The normalization to the  $X$  particle decay width is assumed. For the leading order in  $\alpha_s$  the coefficient functions  $C_i$  are proportional to  $\delta(1-z)$ , and the total spectrum is equal to the sum of fragmentation functions  $F^h(x, s) = \sum_i D_i^h(x, s)$ . Given the fragmentation function at some scale  $s$  we can evolve it to another scale using DGLAP equations [39,40],

$$\frac{\partial D_i^h(x, s)}{\partial \ln s} = \sum_j \frac{\alpha_s(s)}{2\pi} P_{ij}(x, \alpha_s(s)) \otimes D_j^h(x, s), \quad (2)$$

where  $\otimes$  denotes the convolution  $f(x) \otimes g(x) \equiv \int_x^1 dz/z f(z)g(x/z) = \int_x^1 dz/z f(x/z)g(z)$  and  $P_{ij}(x, s)$  is the splitting function for the parton branching  $i \rightarrow j$ . Since we study the process on the scale  $M_X \gg m_q$ , we assume all  $N_f$  quark flavors are coupled to gluon similarly, and we can confine ourselves to considering only the mixing of the gluon fragmentation function with a quark singlet fragmentation function,

$$D_q^h(x, s) = \frac{1}{N_f} \sum_{i=1}^{N_f} [D_{q_i}^h(x, s) + D_{\bar{q}_i}^h(x, s)]. \quad (3)$$

Then DGLAP equations take the form

$$\begin{aligned} \frac{\partial}{\partial \ln s} \begin{pmatrix} D_q^h(x, s) \\ D_g^h(x, s) \end{pmatrix} &= \begin{pmatrix} P_{qq}(x, s) & P_{gq}(x, s) \\ 2N_f P_{qg}(x, s) & P_{gg}(x, s) \end{pmatrix} \\ &\otimes \begin{pmatrix} D_q^h(x, s) \\ D_g^h(x, s) \end{pmatrix}. \end{aligned} \quad (4)$$

In this study we use the code kindly provided by the authors of Ref. [32]. This code evaluates the DGLAP equations numerically in the leading order in  $\alpha(s)$ . We use the initial fragmentation functions from Ref. [38] parametrized on the scale  $M_Z$  and extrapolated to the region  $10^{-5} \leq x \leq 1$ . Although the low  $x$  tail is unreliable at this scale, the results obtained for the high scales  $M_X$  agree with that obtained by Monte Carlo simulation, as was shown in [32]. Fortunately, the spectra calculated in this region of  $x$  are enough to constrain the results with the experiment in the mass range of interest:  $10^7 \leq M_X \leq 10^{16}$  GeV. In this paper we calculate only prompt photon spectra of  $\pi^0$  s decay and neglect the smaller amount of photons from inverse Compton scattering (ICS) of prompt  $e^\pm$  on the interstellar background photons. While for the leptonic decay channels the relative contribution of inverse Compton photons to the full spectrum can be significant [28], for hadronic channels it is at least by order of magnitude lower [36], so we neglect the contribution from prompt  $e^\pm$  via ICS in this study. Following [32] we also neglect roughly 10% contribution of other mesons decay. Then the photon spectrum of the  $X$ -particle decay is given by

$$D^\gamma(x) = 2 \int_x^1 \frac{dz}{z} D^{\pi^0}(z), \quad (5)$$

where  $D^{\pi^0}(x, s) \equiv [D_q^{\pi^0}(x, s) + D_g^{\pi^0}(x, s)]$ . The examples of prompt photon spectra for the decay of  $X$  particles with different masses are shown in Fig. 1.

Having the injected photon spectra we can calculate the corresponding photon flux reaching the Earth. We use the following assumptions. First of all, we neglect the flux coming from the extragalactic region. Starting at

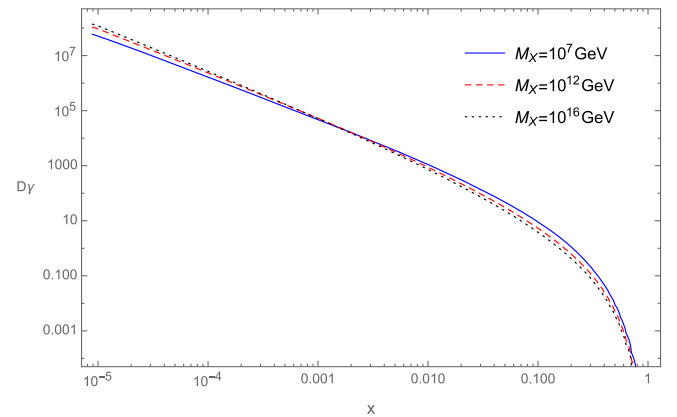


FIG. 1. Prompt photon spectra of  $X$  particle decay.

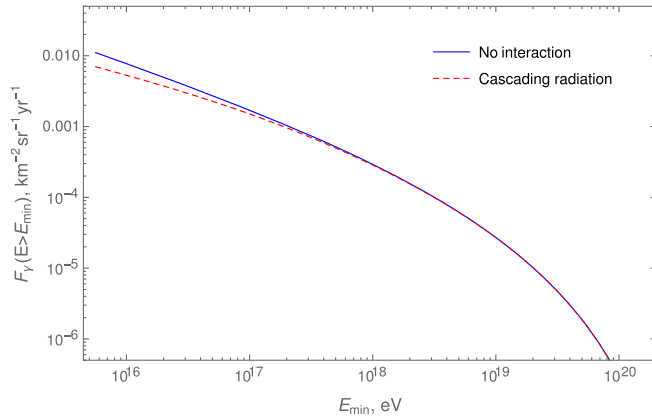


FIG. 2. Integral photon flux from SHDM decay in our Galaxy halo as received by Telescope array experiment,  $M_X = 10^{12}$  GeV, without interactions of photons with a medium (solid line), and with photon interactions with CMB and secondary cascade radiation included (dashed curve).

$E_\gamma = 2 \times 10^{14}$  eV, which is the lowest energy where the EAS experiments provide photon limits, and up to  $E_\gamma \simeq 2 \times 10^{18}$  eV, the photon attenuation length does not exceed the size of our Galaxy halo. Then, up to the highest experimentally tested energy  $E_\gamma = 10^{20}$  eV photons can come from a region of size not exceeding 50 Mpc, of which the contribution to the flux is about 1% of that from our Galaxy [41].

For the galactic photon flux calculation we use Navarro-Frenk-White dark matter distribution [42,43] with the parametrization for the Milky Way from Ref. [36].<sup>2</sup> We assume photons being radiated isotropically in the decay of the  $X$  particle. As was mentioned above, for photons with  $E \gtrsim 10^{18}$  eV the attenuation length in the interstellar medium exceeds the size of our Galaxy halo. This implies that for a higher energy photon we can neglect the absorption and cascaded radiation. Indeed, the comparison of the noninteracting and cascading  $\gamma$  fluxes from our Galaxy (the latter was calculated using the numerical code from Ref. [45]; see below) shows that the discrepancy does not exceed a few percent for  $E = 10^{18}$  eV (see Fig. 2). Therefore we neglect the photon interaction with the medium for  $M_X \gtrsim 10^{14}$  GeV. Using the above assumptions we obtain the following expression for the integral photon flux received by a given cosmic ray observatory:

$$F(E > E_{\min}) = \frac{N(E > E_{\min})}{4\pi M_X \tau} \cdot \frac{\int_V \frac{\rho(R)\omega(\delta, a_0, \theta_{\max})}{r^2} dV}{2\pi \int_{-\frac{\pi}{2}}^{\frac{\pi}{2}} \omega(\delta, a_0, \theta_{\max}) \cos(\delta) d\delta}; \quad (6)$$

<sup>2</sup>For comparison we have also tested the Burkert dark matter profile [44].

where  $\rho(R)$  is a DM density as a function of distance  $R$  from the Galactic center,  $r$  is a distance from Earth,  $\omega$  is a relative exposure of the given observatory, and  $N(E > E_{\min})$  is an integral number of photons with energies higher than  $E_{\min}$  produced in the decay of the  $X$  particle. Integration in the numerator takes over all volumes of halo ( $R_{\max} = 260$  kpc) and in the denominator over all sky (the averaging over right ascension is included in the definition of  $\omega$ ). The relative exposure  $\omega$  is a function of declination  $\delta$ , geographical latitude of the given experiment  $a_0$ , and the maximal zenith angle  $\theta_{\max}$  of particles allowed for observation in this experiment (see Refs. [46,47] for details).

For  $M_X \lesssim 10^{14}$  GeV we also take into account the attenuation of photons on CMB using the numerical code [45]. The code simulates development of electron-photon cascades on CMB driven by the chain of  $e^\pm$  pair production and inverse Compton scattering. Although the code allows one to calculate the flux of the cascade photons, it does not take into account deflections of  $e^\pm$  by the halo magnetic field. Since electrons in the code propagate rectilinearly they produce fewer cascade photons. Therefore the calculated flux of photons should be considered as a conservative lower bound. The propagation code [45] also includes the attenuation of photons on extragalactic background light (EBL), though the effect of EBL is negligible on distances that we consider.

### III. COMPARISON WITH PHOTON LIMITS

Finally we compare the predicted SHDM signal with the existing experimental upper limits on photon flux. For the highest observable cosmic ray energies ( $E_{\text{CR}} \gtrsim 10^{18}$  eV) the recent constraints are provided by Pierre Auger Observatory [17,18], Telescope Array experiment [19], and Yakutsk experiment [20], while for the lower energies we use the results of CASA-MIA [23], KASCADE [22], KASCADE-Grande [21], and EAS-MSU [16]. For a review of experimental results, see, e.g., Ref. [48] and references therein. We should note that the higher energy limits are more effective for constraining SHDM since its decay spectra is quite hard; i.e., the SHDM photon flux grows slower than the experimental limits with the decreasing of energy.

Another possible contribution to ultrahigh energy (UHE) photon flux comes from astrophysics. UHE protons and nuclei produced by extragalactic sources interact with CMB and other interstellar background producing secondary electron-photon cascades and neutrinos. The essentially isotropic flux of photons of this origin has been estimated in several scenarios including proton and nuclei emitting sources (see, e.g., Refs. [49–53]). In contrast to the astrophysical signal, the SHDM contribution is anisotropic with maximum flux arriving from the center of the Milky Way. In Figs. 3 and 4 we show the  $\gamma$ -ray flux limits by KASCADE, KASCADE-Grande, and Pierre Auger Observatory together with predicted SHDM decay photon

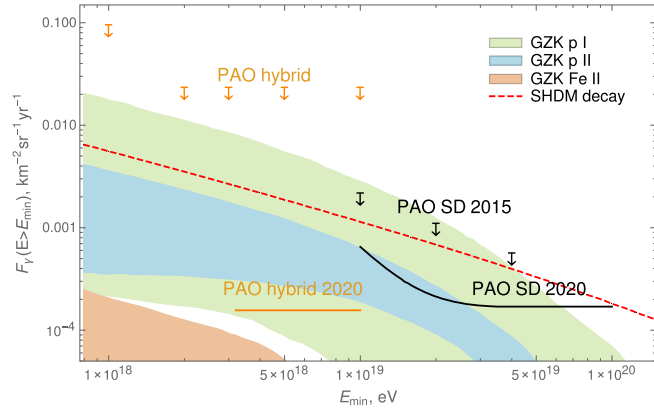


FIG. 3. Predicted integral photon flux from the decay of SHDM with mass  $M_X = 10^{14}$  GeV and lifetime  $\tau = 2 \times 10^{22}$  yr compared with upper limits of Pierre Auger Observatory [17,18] and its estimated sensitivity for 2020 (assuming the upgrade of the facility) [48]. Estimates of the  $\gamma$ -ray background produced by attenuation of UHE protons [49] (green shaded areas) and UHE protons and iron induced cascades [50] (blue and orange shaded areas) are shown with their theoretical uncertainties.

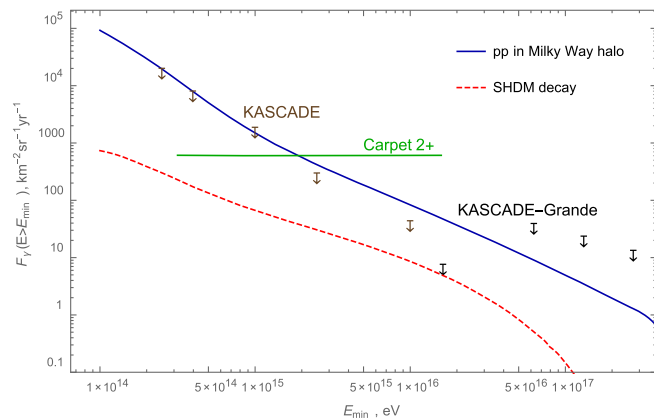


FIG. 4. Predicted integral photon flux from the decay of SHDM with mass  $M_X = 10^9$  GeV and lifetime  $\tau = 3 \times 10^{21}$  yr compared with the upper limits of KASCADE and KASCADE-Grande experiments [21,22], the estimated sensitivity of Carpet 2+ experiment [54], and the estimate [51] of the  $\gamma$  background from  $pp$  interactions in halo.

flux (for certain parameters of SHDM) and some estimates of astrophysical photon flux. Also we show the estimated future sensitivity of Carpet experiment [54] in Fig. 4 and upgraded PAO [48] in Fig. 3.<sup>3</sup>

We compare the constraints of various experiments on SHDM mass and lifetime in Fig. 5. The constraints are built by scanning SHDM parameter space and matching the predicted photon signal with the limits of the given

<sup>3</sup>Because of the strong anisotropy of the predicted SHDM signal, we do not show all the existing experimental limits on a single picture. KASCADE and Carpet experiments have approximately the same geographical latitude.

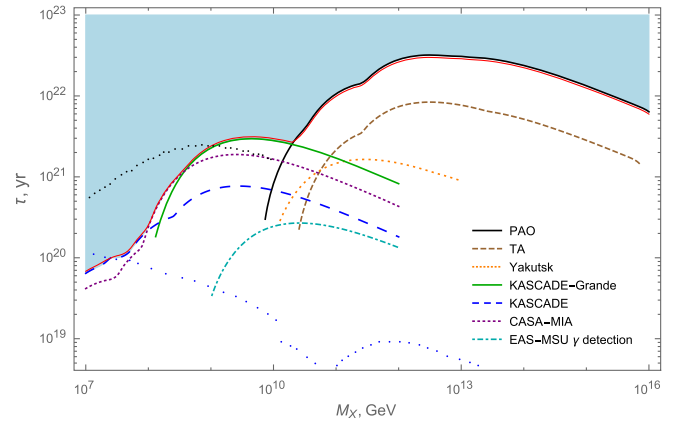


FIG. 5. Constraints on mass  $M_X$  and lifetime  $\tau$  of superheavy dark matter. White area is excluded. For comparison we present the constraints obtained with the Burkert DM profile (solid thin red line). We also show the constraint obtained with neutrino limits: for  $X \rightarrow \nu\bar{\nu}$  channel [55] (blue dots) and for  $X \rightarrow b\bar{b}$  channel [25] (black dots).

experiment. The model is considered as excluded as soon as the signal touches the limit points from below. For the EAS-MSU result of photon detection [16] we show the fit assuming the whole photon flux being produced by SHDM decay. The constraints based on Pierre Auger Observatory limits are the strongest since this experiment has the largest exposure among UHECR experiments, and it is located in the Southern Hemisphere where higher  $\gamma$ -ray flux coming from the Galactic center could be detected. The strongest constraint over all mass range is  $\tau \gtrsim 3 \times 10^{22}$  yr at  $M_X \approx 3 \times 10^{12}$  GeV. It slightly improves the result of Ref. [26] for which the old PAO limits were used. In the low energy region the best constraints are derived from KASCADE, CASA-MIA, and KASCADE-Grande: minimal lifetime increases from  $\tau \approx 6 \times 10^{19}$  yr at  $M_X = 10^7$  GeV to  $\tau \approx 3 \times 10^{21}$  yr at  $M_X = 5 \times 10^9$  GeV being of the same order as the constraints of Refs. [25,27,28] that were obtained in a wider theoretical context. The constraints obtained with Burkert dark matter profile is slightly weaker than that of NFW in the high energy region, where PAO observes the Galactic center, and stronger for low energies, where constraints are put by Northern hemisphere experiments.

It is also interesting to compare our constraints with those obtained from neutrino limits. In Ref. [25] the neutrino constraints on  $\tau$  were imposed for  $M_X < 10^{10}$  GeV and for various decay channels. Our constraints are of the same order as these for  $M_X \gtrsim 10^9$  GeV but become weaker for  $M_X \lesssim 10^9$  GeV. The case of direct decay of dark matter into neutrino was studied in Ref. [55] for a wide region  $10 < M_X < 10^{19}$  GeV. The constraints on  $\tau$  obtained there are of the same order as ours for  $M_X \lesssim 10^8$  GeV and are weaker for all higher masses.

Our constraints have an implication for the EAS-MSU tentative result of 100 PeV gamma detection [16]. We may

see that the curve interpreting it as the product of SHDM decay lies deep in the parameter area excluded by the other experiments, and this implies that the SHDM component in the EAS-MSU photon signal cannot be dominant.

Discussing these results we may note that although the recent experimental limits touch the astrophysically predicted region, due to large uncertainty of astrophysical  $\gamma$ -ray flux, one cannot yet exclude the dominant contribution of SHDM decay. Nevertheless, one might use the guaranteed, i.e., minimal, predicted astrophysical gamma flux to constrain SHDM parameters even stronger. Finally, if  $\gamma$  rays are detected, the discrimination between the astrophysical and the SHDM (or other exotic) origin

scenario could in principle be made by analyzing the flux anisotropy and energy spectrum.

## ACKNOWLEDGMENTS

We thank S. Troitsky and G. Rubtsov for helpful discussions. We are especially indebted to R. Aloisio, V. Berezhinsky, and M. Kachelriess for providing the numerical code solving DGLAP equations. This work has been supported by Russian Science Foundation Grant No. 14-22-00161. Numerical simulations have been performed in part at the computer cluster of the Theoretical Physics Department of the Institute for Nuclear Research of the Russian Academy of Sciences.

- 
- [1] V. A. Kuzmin and V. A. Rubakov, *Phys. At. Nucl.* **61**, 1028 (1998).
- [2] V. Berezhinsky, M. Kachelriess, and A. Vilenkin, *Phys. Rev. Lett.* **79**, 4302 (1997).
- [3] D. Fargion, M. Y. Khlopov, R. V. Konoplich, V. R. Konoplich, and R. Mignani, *Mod. Phys. Lett. A* **11**, 1363 (1996).
- [4] M. Y. Khlopov and V. M. Chechetkin, *Fiz. Elem. Chastits At. Yadra* **18**, 627 (1987).
- [5] E. W. Kolb, D. J. H. Chung, and A. Riotto, in *Dark Matter in Astrophysics and Particle Physics 1998: Proceedings of the Second International Conference on Dark Matter in Astro and Particle Physics, Heidelberg, Germany, 1998* (CRC Press, Boca Raton, 1999), pp. 592–614.
- [6] V. A. Kuzmin and I. I. Tkachev, *Phys. Rep.* **320**, 199 (1999).
- [7] L. Kofman, A. D. Linde, and A. A. Starobinsky, *Phys. Rev. Lett.* **73**, 3195 (1994).
- [8] G. N. Felder, L. Kofman, and A. D. Linde, *Phys. Rev. D* **59**, 123523 (1999).
- [9] D. J. H. Chung, E. W. Kolb, and A. Riotto, *Phys. Rev. D* **60**, 063504 (1999).
- [10] D. J. H. Chung, E. W. Kolb, and A. Riotto, *Phys. Rev. D* **59**, 023501 (1998).
- [11] V. Kuzmin and I. Tkachev, *Phys. Rev. D* **59**, 123006 (1999).
- [12] D. J. H. Chung, E. W. Kolb, A. Riotto, and L. Senatore, *Phys. Rev. D* **72**, 023511 (2005).
- [13] D. S. Gorbunov and A. G. Panin, *Phys. Lett. B* **718**, 15 (2012).
- [14] R. Aloisio, V. Berezhinsky, and M. Kachelriess, *Phys. Rev. D* **74**, 023516 (2006).
- [15] Y. A. Fomin, N. N. Kalmykov, G. V. Kulikov, V. P. Sulakov, and S. V. Troitsky, *J. Exp. Theor. Phys.* **117**, 1011 (2013).
- [16] Y. A. Fomin, N. N. Kalmykov, G. V. Kulikov, V. P. Sulakov, and S. V. Troitsky, *Pis'ma Zh. Eksp. Teor. Fiz.* **100**, 797 (2014) [*JETP Lett.* **100**, 699 (2015)].
- [17] A. Aab *et al.* (Pierre Auger Collaboration), [arXiv:1509.03732](https://arxiv.org/abs/1509.03732).
- [18] P. Abreu *et al.* (Pierre Auger Collaboration), [arXiv:1107.4805](https://arxiv.org/abs/1107.4805).
- [19] G. I. Rubtsov *et al.* (for the Telescope Array Collaboration), *Proc. ICRC* **2015**, 331 (2015).
- [20] A. V. Glushkov, I. T. Makarov, M. I. Pravdin, I. E. Sleptsov, D. S. Gorbunov, G. I. Rubtsov, and S. V. Troitsky, *Phys. Rev. D* **82**, 041101 (2010).
- [21] D. Kang *et al.* (KASCADE-Grande Collaboration), *J. Phys. Conf. Ser.* **632**, 012013 (2015).
- [22] G. Schatz *et al.* (KASCADE Collaboration), *Proceedings of the 28th International Cosmic Ray Conference* (Universal Academy Press Inc., Tokyo, 2003) Vol. 4, p. 2293.
- [23] M. C. Chantell *et al.* (CASA-MIA Collaboration), *Phys. Rev. Lett.* **79**, 1805 (1997).
- [24] O. E. Kalashev, G. I. Rubtsov, and S. V. Troitsky, *Phys. Rev. D* **80**, 103006 (2009).
- [25] K. Murase and J. F. Beacom, *J. Cosmol. Astropart. Phys.* **10** (2012) 043.
- [26] R. Aloisio, S. Matarrese, and A. V. Olinto, *J. Cosmol. Astropart. Phys.* **08** (2015) 024.
- [27] K. Murase, R. Laha, S. Ando, and M. Ahlers, *Phys. Rev. Lett.* **115**, 071301 (2015).
- [28] A. Esmaili and P. D. Serpico, *J. Cosmol. Astropart. Phys.* **10** (2015) 014.
- [29] P. S. B. Dev, D. Kazanas, R. N. Mohapatra, V. L. Teplitz, and Y. Zhang, *J. Cosmol. Astropart. Phys.* **08** (2016) 034.
- [30] M. G. Aartsen *et al.* (IceCube Collaboration), *Science* **342**, 1242856 (2013).
- [31] V. Berezhinsky and M. Kachelriess, *Phys. Rev. D* **63**, 034007 (2001).
- [32] R. Aloisio, V. Berezhinsky, and M. Kachelriess, *Phys. Rev. D* **69**, 094023 (2004).
- [33] S. Sarkar and R. Toldra, *Nucl. Phys.* **B621**, 495 (2002).
- [34] C. Barbot and M. Drees, *Phys. Lett. B* **533**, 107 (2002).
- [35] C. Barbot and M. Drees, *Astropart. Phys.* **20**, 5 (2003).
- [36] M. Cirelli, G. Corcella, A. Hektor, G. Hütsi, M. Kadastik, P. Panci, M. Raidal, F. Sala, and A. Strumia, *J. Cosmol. Astropart. Phys.* **03** (2011) 051; **10** (2012) E01.
- [37] P. Ciafaloni, D. Comelli, A. Riotto, F. Sala, A. Strumia, and A. Urbano, *J. Cosmol. Astropart. Phys.* **03** (2011) 019.
- [38] M. Hirai, S. Kumano, T.-H. Nagai, and K. Sudoh, *Phys. Rev. D* **75**, 094009 (2007).

- [39] V. N. Gribov and L. N. Lipatov, *Sov. J. Nucl. Phys.* **15**, 438 (1972); L. N. Lipatov, *Sov. J. Nucl. Phys.* **20**, 94 (1975); Yu. L. Dokshitzer, *Sov. Phys. JETP* **46**, 641 (1977).
- [40] G. Altarelli and G. Parisi, *Nucl. Phys.* **B126**, 298 (1977).
- [41] S. L. Dubovsky and P. G. Tinyakov, *JETP Lett.* **68**, 107 (1998).
- [42] J. F. Navarro, C. S. Frenk, and S. D. M. White, *Astrophys. J.* **462**, 563 (1996).
- [43] J. F. Navarro, C. S. Frenk, and S. D. M. White, *Astrophys. J.* **490**, 493 (1997).
- [44] A. Burkert, *IAU Symp.* **171**, 175 (1996); *Astrophys. J.* **447**, L25 (1995).
- [45] O. E. Kalashev and E. Kido, *J. Exp. Theor. Phys.* **120**, 790 (2015).
- [46] P. Sommers, *Astropart. Phys.* **14**, 271 (2001).
- [47] A. Aab *et al.* (Telescope Array and Pierre Auger Collaborations), *Astrophys. J.* **794**, 172 (2014).
- [48] T. Karg *et al.* (IceCube and Pierre Auger and Telescope Array Collaborations), *J. Phys. Soc. Jpn. Conf. Proc.* **9**, 010021 (2016).
- [49] G. Gelmini, O. E. Kalashev, and D. V. Semikoz, *J. Exp. Theor. Phys.* **106**, 1061 (2008).
- [50] D. Hooper, A. M. Taylor, and S. Sarkar, *Astropart. Phys.* **34**, 340 (2011).
- [51] O. E. Kalashev and S. V. Troitsky, *JETP Lett.* **100**, 761 (2015).
- [52] M. Ahlers and K. Murase, *Phys. Rev. D* **90**, 023010 (2014).
- [53] J. C. Joshi, W. Winter, and N. Gupta, *Mon. Not. R. Astron. Soc.* **439**, 3414 (2014); **446**, 892(E) (2015).
- [54] D. D. Dzhappuev, V. B. Petkov, A. U. Kudzhaev, N. F. Klimenko, A. S. Lidvansky, and S. V. Troitsky, [arXiv:1511.09397](https://arxiv.org/abs/1511.09397).
- [55] A. Esmaili, A. Ibarra, and O. L. G. Peres, *J. Cosmol. Astropart. Phys.* **11** (2012) 034.